# Limitations and Guidelines for Damage Estimation Based on Lifetime Models for High-Power IGBTs in Realistic Application Conditions

Antonios Antonopoulos, *Member, IEEE,* Salvatore D'Arco, Magnar Hernes, and Dimosthenis Peftitsis, *Senior Member, IEEE*

***Abstract*—Statistical lifetime models for high-power IGBTs are developed based on results from power-cycling experiments, and relate lifetime expectancy to the well-defined conditions of a laboratory experiment. In most cases, predefined cyclic-stress conditions are repeatedly applied, until the power device under test reaches its end of life. However, in real applications, power modules are exposed to non-repetitive stress patterns that can be very different from the power-cycling conditions. A well established lifetime-estimation method suggests to decompose the stress pattern into individual components, whose damage can be calculated using a lifetime model. These damage contributions are then summed up in order to estimate the consumed or the remaining lifetime of a device. When comparing the estimation results to field measurements though, they often fail to match the real behaviour of a power device. This paper points out the uncertainties that appear in this process of applying a lifetime model on stress patterns deriving from field applications. The main purpose is to present typical sources of errors, and discuss how severely these may impact the lifetime estimation.**

## I. Introduction

Power-cycling experiments are a widely accepted and useful approach to evaluate the durability of power-electronic devices. In these experiments, a predefined temperature (or current) profile is applied to the device under test, causing the desired temperature variation, and the device lifetime is assessed using the maximum number of cycles it can sustain before reaching its end-of-life condition. Collecting results from a large number of such experiments on different device samples, and also under various current, die-heating times, and temperature combinations, allows for a more comprehensive lifetime modelling of power devices. Modeling efforts are described in literature [1], [2], and comprise a useful tool to compare power devices, especially when lifetime becomes an important design aspect.

The most widely used lifetime models are the results of statistical analyses on large numbers of failed device samples, and not models directly describing physical causality of the failure [3]. The factors that affect lifetime are defined in each model based on empirical knowledge. However, the exact contribution of each factor to the resulting lifetime is reflected through a number of coefficients, which are determined by applying statistical methods on experimental results performed for a variety of test conditions. Moreover, it has been pointed out that there may be strong correlation between some of these factors [2], [4], which limits the reliability of these results when interpolating or extrapolating to operating points that are different than the ones actually tested in the power-cycling characterization.

Power-electronic devices operating in commercial applications are suffering varying temperature profiles, as they are exposed to a variety of ambient and load conditions. Even if, in some cases, there is sufficient information available to construct the expected temperature profile of a device over a full calendar year of operation [5]–[7], it is not feasible to test these profiles in a dedicated power-cycling test [8]. However, the data associated to a mission profile can be analysed and decomposed into elementary stress cycles with well specified parameters e.g. temperature variation, minimum temperature, pulse width, and load current. The damage contribution of each of these elementary stress components can be calculated by a lifetime model based on the recorded durability of the device from the power-cycling testing. The accumulated damage on each device over the duration of a given mission profile can be then obtained offering also an estimation for the expected (or remaining) lifetime. Numerous recent publications follow this methodology to estimate the lifetime of power converters in different applications [5], [6], [9]–[11].

Lifetime models produce a very reliable and accurate estimation of the lifetime of components when subjected to repetitive stress cycles within their range of validity. This is due to the relatively low tolerances in the present manufacturing processes that translates into small statistical deviations between the individual components. However, while the approach briefly described above could be assumed as the state of the art for assessing lifetime in non-repetitive conditions, still it is very difficult to quantify the error margins between the lifetime predictions, and what could be expected in the real application. In this perspective, there is no sufficient available data in the technical literature for power devices, while in mechanical engineering applications the error is assumed to be within 30% [12]. Nowadays, it is increasingly important to be able to estimate the expected lifetime of the power electronic devices given a mission profile. As an example, converters in offshore installations have limited accessibility, but continuity of service is essential. Despite the possible margins and inaccuracies involved, the methodology for lifetime estimation is very valuable, and typically applied in both academic and industrial context to provide an indicative expected lifetime. An additional benefit of this method is the enhanced estimation it provides, due to the possibility to take into account variations

in the converter hardware design or its control [13]–[15].

The methodology described above involves several steps, like the decomposition of a waveform into cycles, the damage calculation for each cycle component, and the cumulation of these contributions. These steps are relatively sensitive to incorrect assumptions, inaccuracies and noise in the data, and possible misinterpretations that may negatively affect the result. The aim of this paper is to point out limitations and typical sources of errors, and discuss how severely these factors may impact the lifetime estimation in order to facilitate the correct use of this approach for lifetime estimation.

The paper is organized with the following structure: It starts with a description of the steps applied to calculate the remaining lifetime of a device together with a brief presentation of the most widely applied lifetime models. In Section III, a field application is defined, and the methodology is applied to estimate the device lifetime under these operating conditions. In Sections IV-VIII the impact of a number of factors (e.g. the accuracy of the temperature sensor, the effect of very frequent variations, the application of lifetime models, etc) is discussed. Finally, in Section IX all considerations discussed in the paper are consolidated into guidelines that aim to improve the accuracy of the lifetime-estimation results.

## II. Methodology to Estimate Lifetime in Realistic Applications

A methodology to calculate the accumulated fatigue on a mechanical component was developed in the 1960's [12], [16]. Lifetime models could at that time only describe (quite accurately though) the mechanical strength of a material under cyclic application of a given stress/strain force. The breakthrough was to expand fatigue calculation to varying stress conditions, which could realistically represent the mission profile that a component faces during its operational lifetime.

IGBT power modules also suffer from end-of-life failures, and the underlying mechanism for these failures is very similar to the mechanical applications: material fatigue. Fatigue accumulates on joints within the packaging of a power device due to the stress/strain forces that develop between material layers that expand and contract with different thermal coefficients. Expansion and contraction movements occur due to the temperature differences that develop in the structure during operation, e.g. when losses are created on the silicon die. In an effort to calculate the fatigue accumulated in a power device (and ultimately estimate its residual lifetime), it is reasonable to develop a process based on the aforementioned methodology. However, the mechanical stresses on these junctions and interfaces between the different material layers would be very difficult to track. Thus, a pragmatic alternative approach is to measure or estimate the temperature on the silicon die which is the cause of these stresses. Accordingly, lifetime models for power devices are not developed to relate lifetime to cyclic application of stress/strain forces, but (mainly) to junction-temperature variations. A well-established methodology to estimate lifetime for power devices in operation is outlined in Fig. 1, based on the appropriate modifications of the methodology developed for mechanical applications.

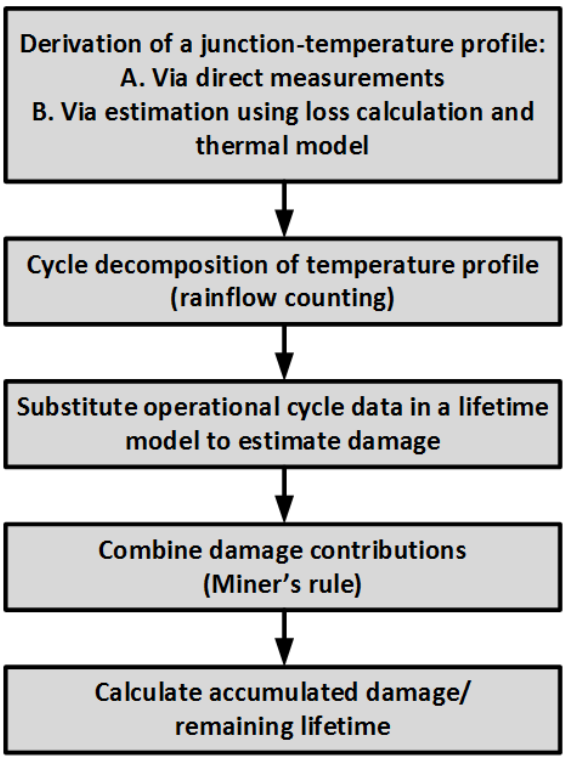


Fig. 1. Methodology to estimate lifetime based on a mission profile.

### A. Derivation of junction temperature profile

End-of-life failures of IGBT modules are associated to thermo-mechanical stress caused by variations in the junction temperature. The first step of the methodology aims at deriving the junction-temperature profile when the device is running a mission profile. A first approach consists in estimating the device losses, and then import these losses in a dynamic thermal model of the device (e.g. Cauer or Foster network). Switching and conduction losses can be calculated knowing the current and voltage applied to the device and the switching pattern. The necessary parameters for this evaluation (e.g. conduction resistance, switching energies and thermal network resistances and capacitances) can be determined experimentally or obtained from the datasheet of the device. As an alternative the junction temperature can be measured directly, or indirectly through measurements of thermal-sensitive parameters, as the gate-emitter voltage.

### B. Decomposition in elementary cycles

A temperature waveform that is generated in field-application conditions leads, in general, to a non-repetitive profile for the junction temperature. This is very dissimilar from the conditions applied during the power-cycling testing for characterizing the devices. Before further processing, the profile needs to be decomposed into elementary closed cycles

that represent a heating phase, where the device temperature rises, followed by a cooling phase where the temperature decreases until the initial temperature (returning to the initial temperature characterizes the cycle as "closed"). These cycles are normally defined by four parameters: the temperature variation $\Delta T_j$ as the difference between the maximum and minimum temperature, the average cycle temperature $T_{j,avg}$, the time duration of the cycle, and the rise time to reach the maximum temperature. It should be noticed that the cycles are assumed to be superimposed and intertwined and not sequential. The decomposition into elementary cycles should be performed by what are referred as "cycle-counting" algorithms or counting methods [12]. These methods have originated from analysis of fatigue damage in aeronautical structures, and then extended to other application areas. A very common cycle counting algorithm is the rainflow counting or pagoda-roof method introduced in 1968 [16], and further revisited and enhanced in the following years to become a standard practice [17]. The name originates from visual analogies of the counting process with rain drops falling on a pagoda-shaped roof. The rainflow counting has nowadays been commonly applied in the decomposition of thermal stresses for power-electronic devices [5]–[7], [9], [18], and is assumed as the reference for cycle counting in this paper.

### C. Lifetime Models for High-Power IGBTs

Having a waveform decomposed in elementary cycles, the next step is to estimate the damage each of these cycles create. A lifetime expression is therefore necessary to relate the data retrieved from the cycle counting into damage contributions. Lifetime models have been developed based on large numbers of experimental data from power-cycling tests. During each test, the devices are exposed to a loading scenario that is repeated until the devices meet certain end-of-life criteria [4]. In each loading scenario, the operational characteristics of the test are varied, in order to achieve different stress conditions. Collecting results from several loading scenarios, and possibly a number of different devices, allows for the development of generic statistical expressions, trying to express the dependence of the device lifetime on the operational conditions it has been exposed to. An example of such a lifetime expression is given in

$$N_f = A \cdot {\Delta T_j}^{\alpha} \cdot \exp\left(\frac{Q}{R \cdot T_m}\right), \tag{1}$$

which is the conclusion of [1] (often referred as the LESIT model in literature). In this expression, $N_f$ is the expected lifetime of a device (in number of cycles) exposed to junction-temperature variations of peak-to-peak amplitude $\Delta T_j$ with a mean temperature $T_m$. The coefficients $A$ and $\alpha$ are device specific, while the parameters $Q$ and $R$ are physical constants.

In efforts to analyse deeper the ageing mechanism of power devices, it has been observed that a greater number of parameters are involved, which are affecting the device lifetime in different ways. A well-acknowledged effort to include the impact of more parameters has been described in [2] (often referred as the CIPS'08 model in literature), where the lifetime expression described has been expanded as

$$N_f = K \cdot {\Delta T_j}^{\beta_1} \cdot \exp\left(\frac{\beta_2}{T_{j,\min} + 273}\right) \cdot {t_{\text{on}}}^{\beta_3} \cdot {I}^{\beta_4} \cdot {V}^{\beta_5} \cdot {D}^{\beta_6}. \tag{2}$$

According to this expression, the lifetime of a device (in number of cycles) depends on six parameters: the junction-temperature swing $\Delta T_j$, the minimum junction temperature of each swing $T_{j,\min}$, the time it takes for the temperature gradient to build up $t_{\text{on}}$, the current per bond foot $I$, the blocking voltage of the chip $V$, and the bond-wire diameter $D$. Actually, the mechanical stresses that develop in a device are a result of the combination of the operational and the structural characteristics of the device, described by these parameters. Each one of these parameters contributes with a different $\beta_i$-coefficient to the device ageing.

It is reasonable to expect that there may be differences in the calculated lifetime, based on the expression used as the lifetime model. A comprehensive analysis for the impact of the model selection can be found in [19]. The aim of this paper is to show that the model selection is only one among many factors that can cause significant inaccuracy in the lifetime estimation process, so the investigation is limited to the aforementioned models.

### D. Cumulative Damage Estimation

The aforementioned models express the expected lifetime of a device when this suffers the same cyclic stress throughout its whole lifetime. If the device is exposed to a number of different stress components, a reasonable way to combine the damage contributions from these is described in

$$\text{Damage} = \sum_{f=1\ldots k} \frac{n_f}{N_f}, \tag{3}$$

where the contribution of each stress component $n_f$ is weighted by the expected lifetime of the device, under the continuous stress of this single component, as estimated using the lifetime models described above. This is widely known as "Miner-Palmgren's rule" [20], and suggests there is linear accumulation of damage from each stress contribution. The device is expected to reach its end-of-life when the accumulated damage reaches unity [12].

## III. Lifetime Estimation Based on Field Application Data

### A. Laboratory setup

In order to discuss the impact of different parameters, data from a field-application example are generated and processed. The application considered here is a high-voltage direct-current (HVDC) transmission, with converter stations based on the Modular Multilevel Converter (MMC) technology. The converter is implemented using half-bridge submodules, as in Fig. 2.

The application conditions are generated in a lab environment, where a downscaled hardware converter is implemented,

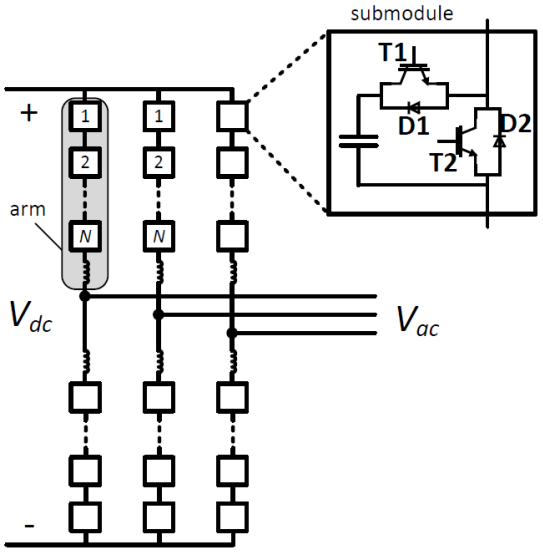


Fig. 2. Circuit outline of a 3-phase MMC, implemented with half-bridge submodules.

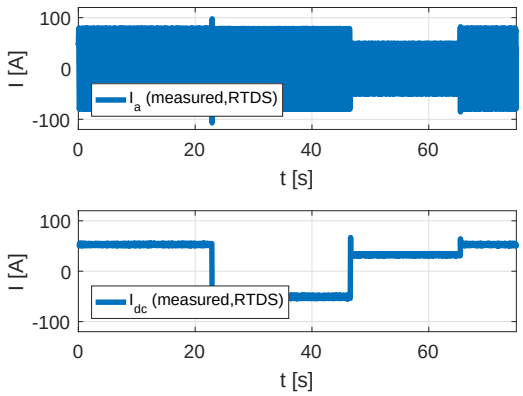


Fig. 3. Phase and dc-side currents showing the load variations during a 75-second long test of an MMC-HVDC converter.

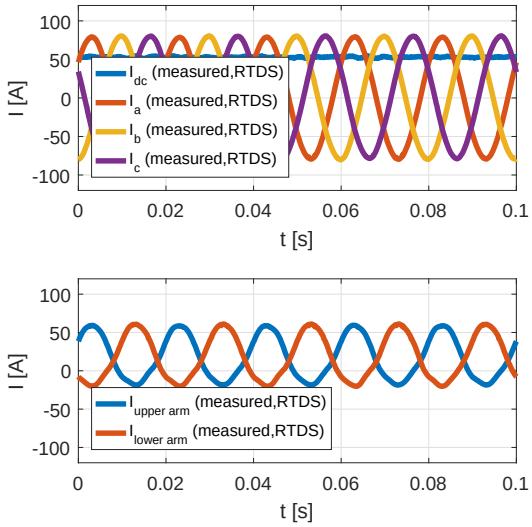


Fig. 4. Detail showing the phase, dc-side, and arm currents at an instant of the laboratory experiment.

and the ac- and dc-side networks are simulated in a real-time digital simulation system. The converter is running a 75-second-long load profile, with phase, dc-side, and arm (or device) currents as shown in Figs. 3 and 4. The laboratory setup offers also a concrete example of how the reliability assessment based on cycle counting could be implemented in a converter for on line assessment of the residual lifetime. It should be noted that the junction temperature could have been obtained also from numerical simulations by combining a very detailed switching model of the converter with a thermal model of the devices. However, this laboratory implementation provided results in real time with possibly a few orders of magnitude decrease in the computation time compared to simulations.

The voltage and current measurements are scaled to the values corresponding to the HVDC-rated converter shown in Table I. These values and the switching state of the devices are then utilized to calculate power losses. Conduction losses are obtained from the instantaneous current, and a tabulated value for the collector-emitter voltage drop, at the expected temperature. The switching losses are obtained by adding up tabulated values for switching energy at turn-on and turn-off instants for each switching event. These tabulated values for the collector-emitter voltage drop and the switching energies as functions of the voltage, the currents, and the temperature are derived from the device datasheet. The total power losses are then fed into a Foster thermal model for the 3.3-kV commercial IGBT power module used to evaluate the situation in a high-voltage application. The parameters of the thermal network are obtained based on the datasheet specifications. Finally, the junction temperature is calculated in real time by an FPGA implementing all the aforementioned calculations.

Given that the IGBT device considered here is rated for 1 kA RMS current, the IGBTs are moderately loaded. The temperature profile for the high-power IGBTs is created in real time, simultaneously as the experiment is performed on the laboratory scale converter. The converter control and temperature estimation process is outlined in Fig. 5, and the temperature waveforms for the examined load profile, corresponding to the four devices (two IGBTs and two diodes) of one (HVDC-rated) converter submodule, are shown in Fig. 6.

### *B. Process - Methodology*

The lifetime-estimation methodology is based on processing a device-temperature waveform. This waveform is analyzed into elementary temperature-variation components reflecting the stress/strain forces, which wear down the different joints in the device packaging structure. Rainflow counting provides a tool to analyze a randomly-varying stress waveform into

TABLE I
LABORATORY EXPERIMENTAL VALUES AND SCALING TO HVDC APPLICATION VALUES.

| Scaling factors | | |
|---|---|---|
| Voltage scaling | 15x | |
| Current scaling | 10x | |
| **Voltage values** | | |
| | Lab experiment | HVDC application |
| Submodule capacitor average voltage | 120 V | 1.8 kV |
| # of submodules per arm | 6 | $N$ |
| dc-link voltage | 720 V | $N$·1.8 kV |
| ac-side amplitude modulation index $m_a$ | 0.889 | 0.889 |
| Peak output (ac-side) voltage | 320 V | 0.5·$N$· 0.889 ·1.8 kV |
| **Maximum Current values (lab rating limited)** | | |
| Peak output (alternating) current | 80 A | 800 A |
| direct current | 53.3 A | 533 A |
| Peak device (arm) current | 57.8 A | 578 A |
| RMS device (arm) current | 33.4 A | 334 A |

individual stress components [16], [17]. The analysis considered in this paper utilizes a real-time implementation of the rainflow-counting algorithm [21], and the damage contribution of each variation is evaluated using the lifetime model in (2). The contributions of all damage components are summed together using Miner's rule to get the accumulated damage on the device material, which also reflects the remaining lifetime of the device.

An application of this process to the waveform of the device T1 from Fig. 6 gives an estimated lifetime of 10.8 years for the 3.3-kV IGBT device in consideration. The lifetime model used to obtain this result is the one in (2). In order to obtain representative $\beta_i$ coefficients for the device under consideration, a number of 3.3-kV IGBT devices underwent power-cycling experiments in the laboratory. The devices were exposed in a number of different $\Delta T_j$s, $t_{\text{on}}$ times, and currents, keeping the $T_{j,\min}$ always at 60°C. The coefficients were then obtained by least-square fitting the results of this experimentation, and are shown in Table II. These coefficients are dedicated for the power module under investigation, and are used for its lifetime estimation in the aforementioned application. It is worth pointing out that there is significant difference in the values of the coefficients adapted to the specific 3.3-kV IGBT module, compared to the ones presented in [2]. This is justified by the fact that the tests performed here concern only one specific module technology, which would lift the uncertainties related to a spread in the structural characteristics (breakdown voltage, bond-wire diameter), and also there are certain technology improvements since the time [2] was published. At the same time, this difference in

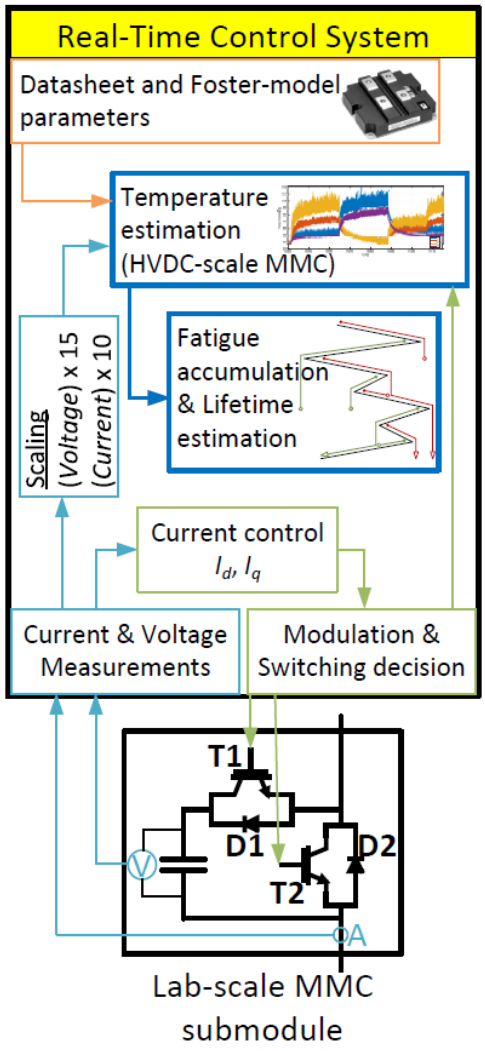


Fig. 5. Outline of the real-time control and calculation process.

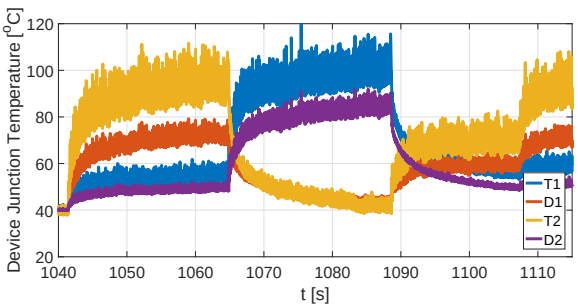


Fig. 6. Temperature waveforms for the IGBTs and diodes of an HVDC converter, running the load profile shown in Fig.3, scaled up to the real-application conditions.

the coefficient values may considerably affect the estimation results compared to the original coefficients. As there is only one module under investigation, the exponents referring to the chip thickness and the bond-wire diameter are not changing,

so they can be incorporated in the factor $K_{eq}$. However, in this process there is a number of factors that can affect the estimation results, with different significance in each case. The impact of these factors will be analysed in the following, based on an example where the temperature-sensor accuracy is compromised.

TABLE II
COEFFICIENTS OF THE ORIGINAL MODEL IN [2], AND FOR ITS ADAPTATION TO THE 3.3-KV IGBT POWER MODULE UNDER INVESTIGATION.

| Original model coefficients in [2] | | | |
|---|---|---|---|
| $K$ | | $\beta_1$ | $\beta_2$ |
| $9.3 \cdot 10^{14}$ | | $-4.416$ | $1.285 \cdot 10^3$ |
| $\beta_3$ | $\beta_4$ | $\beta_5$ | $\beta_6$ |
| $-0.463$ | $-0.716$ | $-0.761$ | $-0.5$ |
| **Adapted coefficients for the 3.3-kV IGBT power module under investigation** | | | |
| $K_{eq} = K \cdot V^{\beta_5} \cdot D^{\beta^6}$ | | | $\beta_1$ |
| $9.34 \cdot 10^{20}$ | | | $-2.07$ |
| $\beta_2$ | | $\beta_3$ | $\beta_4$ |
| $0.713 \cdot 10^3$ | | $-1.42$ | $-4.1$ |

## IV. TEMPERATURE SENSOR/ESTIMATOR ACCURACY

The first contributing factor to the uncertainty of the results is the accuracy of the temperature sensors. In the example described above, the junction temperature is estimated in real time, using a loss model for the devices, together with a Foster model of the packaging structure. The junction temperature can also be measured using a variety of methods in an application (direct measurement, device on-state voltage, etc.) [22]. However, either the junction temperature is estimated or even measured, there is a certain error in this estimation/measurement. This error derives partially from modelling imperfections or measurement inaccuracies. On large device surfaces, used in high-current applications, it is observed that there may be a temperature difference of a few degrees among different points on the same device surface [23]. It is, therefore, hard to expect that a junction-temperature measurement or estimation will give a decimal-digit accuracy. A few $^{o}$C of inaccuracy are within the reasonable limits for a junction-temperature measurement; however, this measurement error should not cause significant impact on the validity of the results.

To expose the sensitivity of the lifetime-estimation result in small inaccuracies of the temperature sensors, the temperature waveforms from Fig. 6 are saved and reprocessed offline, polluted this time with a component to represent a certain fault in the sensor. In the first two cases, the sensor fault is considered to be always in the same direction: either the sensor over- or underestimates the actual temperature on the device by 5$^{o}$C. In the third case, the temperature signal is polluted with a white-noise component, which is added to all the obtained samples. This white noise has always zero mean value, and a maximum amplitude of 1$^{o}$C. The initial and the polluted waveform for one of the IGBT devices in the submodule are shown in Fig. 7. The polluted waveform is processed again with the same procedure, using the exact same parameters, and the resulting estimation for the lifetime is presented in Table III.

TABLE III
EFFECT OF TEMPERATURE SENSOR/ESTIMATOR FAULT ON LIFETIME ESTIMATION RESULTS.

| | |
|---|---|
| Original waveform | 10.8 years |
| Original waveform + 5$^{o}$C | 10.5 years |
| Original waveform - 5$^{o}$C | 11.1 years |
| Original waveform + rand $\in [-1, +1]^{o}$C | 14.3 years |

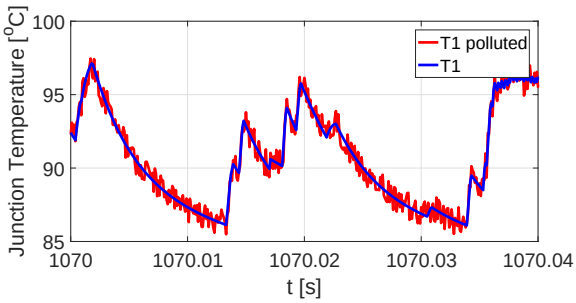


Fig. 7. Detail of the estimated temperature of an IGBT junction in the examined application, polluted with a white-noise component of a maximum temperature of $\pm 1$ $^{o}$C.

A certain fault in the temperature sensor that is always in the same direction affects the minimum temperature of each variation $T_{j,\min}$, and gives a reasonably small inaccuracy in the estimation. A much smaller variation that appears as white noise in the signal, should not affect the results significantly. However, the results indicate the opposite trend. It can be seen already from the output of the rainflow-counting algorithm that this small disturbance in the temperature signal may slightly modify the distribution of the $\Delta T_j$ (or range) values at the output of the rainflow-counting process. In fact, the existence of noise in the waveform disturbs the rainflow counting, which may miscalculate the actual starting/ending points and the duration of each stress cycle. As the lifetime models have exponential dependency on some operational variables (e.g. $\Delta T_j$), small differences in the parameter values may result in very different damage calculations. This can affect both low- and high-temperature variations, and it is not clear if this effect is more evident on high- or low-temperature cycles. The output of the rainflow-counting for the original and the polluted waveform are shown in Figs. 8a and 8b. It is remarkable that a small randomly-varying disturbance with a zero mean value, which can occur in reality (e.g. due to noise disturbances), and affects mostly the amounts of cycles with low $\Delta T_j$s, has such a severe impact on the lifetime estimation. This is a first indication of the vulnerability of the method in consideration, and in the following, a number of factors that can further

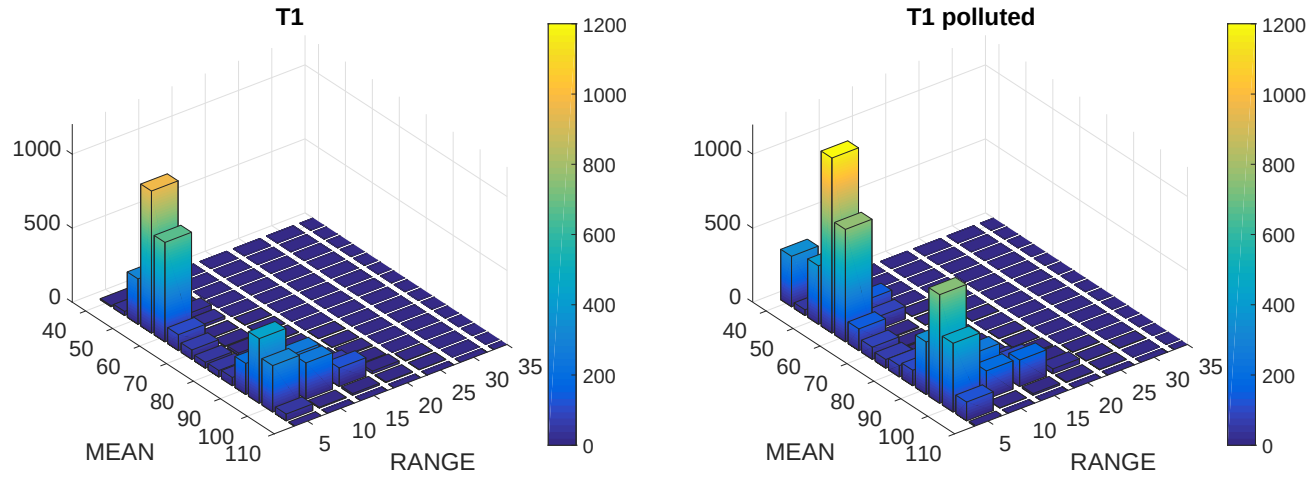


(a) Rainflow-counting output for the original waveform of T1.

(b) Rainflow-counting output for the T1 temperature waveform, polluted with a (maximum) $\pm 1$ °C white noise.

Fig. 8. Rainflow-counting algorithm output for the temperature waveforms shown in Fig. 7. The height of the bars represent the number of cycles counted for each combination of average temperature (MEAN) and temperature difference $\Delta T_j$ (RANGE). The scale of the vertical (z) axis is represented in the coloured bar on the side of each graph.

increase the uncertainty of the results are discussed.

## V. Impact of Small Temperature Variations (in the Elastic Stress Range)

One important aspect appears already when processing the temperature waveform. In mechanical engineering applications, where this lifetime estimation procedure is applied to calculate the accumulated fatigue, rainflow counting is applied directly on the waveform that describes stress/strain forces. In power-device lifetime estimation, in contrast, rainflow counting is applied on the temperature waveform, which is not directly identical to the stress forces. Temperature variations are actually the cause of expansion and contraction, which develops mechanical forces between the different material layers. Furthermore, in stress/strain mechanics there is also a distinction between cyclic elastic and plastic stress, with the former type of stress resulting in virtually zero damage.

However, in power-device applications it is very difficult to define a threshold between cyclic elastic and plastic variations only from the temperature data. The most relevant approach is by thermo-mechanical fatigue analysis, which is hard to support experimentally, due to the long duration of experiments. An effort to define this border between the cyclic-elastic and plastic stress in case of power-device material fatigue is made in [24]. Plastic stress is the result of a combination of certain conditions: significant peak-to-peak temperature variations, at a quite high mean temperature value. As an example, according to the graphs in [24], the impact of a cyclic 30°C variation at a mean temperature of 100°C causes plastic stress, and therefore, material fatigue, while the same cyclic variation at a mean temperature of 40°C is expected to cause only elastic deformation.

Applying the cut-off line shown in [24] on the output of the rainflow-counting algorithm for the temperature of T1, all temperature variations identified by this algorithm are falling into the elastic range, which suggests an infinitely long lifetime for an HVDC converter running the load profile discussed earlier. This is obviously unrealistic. This result, however, emphasizes that data found in the literature should not be applied without criticism.

It is obvious that a similar cut-off line characterising the 3.3-kV device under investigation exists, but may be different than the one shown in [24]. However, it is not easy to define a dedicated limit line for every device experimentally, as a large number of (very long duration) power-cycling experiments need to be performed to provide a clear picture for this low temperature variation range, in order to confirm this behaviour.

## VI. Impact of Certain Assumptions During Processing of a Temperature Waveform

A rainflow-counting algorithm applied on a temperature waveform, like the one in Fig. 6, can give information on many different characteristic values of this waveform. The output data set of the rainflow-counting algorithm contains three parameters that identify each transient: the temperature difference $\Delta T_j$, the minimum (it can also be average or maximum) junction temperature of the transient $T_{j,\min}$, and the duration while this stress application has been active, which reflects $t_{\text{on}}$. It can also identify the direction of the temperature variation, distinguishing the variations into heating half-cycles and cooling ones.

Processing a temperature waveform that represents a periodic variation during a power-cycling experiment, as the one shown in Fig. 9, is rather straightforward: it contains (half-cycle) heating transients of $\Delta T_j$ equal to 70°C, starting from a minimum junction temperature $T_{j,\min}$ of 60°C, and the duration of each heating transient is 0.75s. This is in agreement with the output of the rainflow-counting algorithm processing

this waveform. The algorithm would further indicate that there are equally many (half-cycle) cooling transients, with the same amplitude of 70°C, ending up at a minimum junction temperature $T_{j,\min}$ of 60°C, and the duration of each cooling transient is 2.25s.

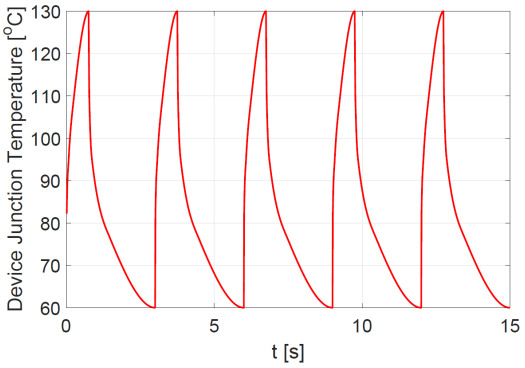


Fig. 9. Junction-temperature waveform during the ideal power-cycling experiment conditions.

### A. *Effect of on-times*

In mechanical applications, the time a stress/strain force is applied does not give any difference to the resulting fatigue. It is the deformation of the material that creates forces, and the cyclic application of these forces causes the material strength to deteriorate. This is the reason why the waveform that is processed in mechanical applications is often simplified to a series of turning points, keeping only the peaks, and damping all information related to times/durations. In power-device lifetime estimation, however, the stress/strain forces and the deformation are not apparent in the lifetime models. Mechanical forces between the material layers are the result of material deformations, which are, in turn, caused by the actual temperature levels and the temperature gradients that develop in the material structure. As heat transfer is a gradual process, the deformation of different layers develops in relation to the duration a heat source is apparent in the structure. Consequently, the mechanical stress that develops is not a direct relation to a (junction) temperature level, but also depends on the duration this (junction) temperature is apparent. Different durations allow different temperature gradients to develop in the material, and as a result, the resulting fatigue from a certain temperature level is different depending on the duration this temperature is apparent: short on-times do not have the same stress impact as long ones. Therefore, the mechanical forces that develop between the different material layers may eventually differ, even if the (measured) junction temperature is the same in terms of $\Delta T_j$ and $T_{j,\min}$.

It is mentioned in [2], [4] that lateral temperature gradients in the material structure cannot fully develop when the on-times are short (<1 s), and this led the authors in [2] to include the impact of $t_{\text{on}}$ in the lifetime model. The important question that arises is how to identify the correct on-time effect in a waveform that derives from real application conditions, which has an almost random behaviour compared to the periodic ones that represent the conditions in a controlled lab experiment. It is absolutely essential to keep the original temperature waveform, and not pass it through any filtering process that keeps only the turning points (which is common in rainflow counting for other applications), as any information related to the duration of the transients would be lost.

The first step to identify the correct on-times in the temperature waveform is to investigate how rainflow counting is actually working. In order to identify the total applied stress on a material, rainflow counting is not terminating every flow at the next possible signal reversal, but it is keeping flows open, until a more significant source appears (deeper valley or higher peak). This means that in order to calculate the correct stress, a flow may remain open through several consecutive signal reversals. Most of this time the flow remains inactive, until it hits the next slope on the waveform. Obviously, the time during this flow is inactive, should not be taken into account, but different parts of active times that have to be accumulated may be several milliseconds (or even seconds) apart. An example of this situation is given in Fig. 10.

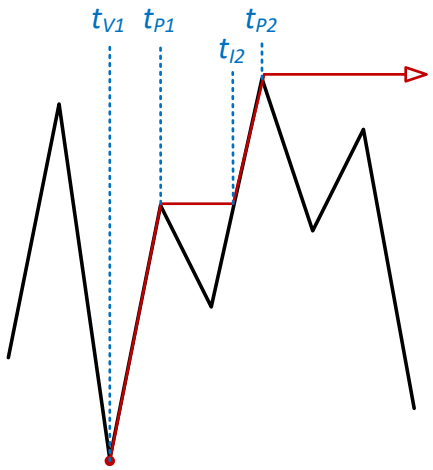


Fig. 10. Example of a flow that continues beyond the nearest signal reversal: In this case $t_{\text{on}}$ should be equal to $(t_{P1} - t_{V1}) + (t_{P2} - t_{I2})$.

Spreading the active time of a stress component into several parts may give a more representative calculation of the on-time; however, it reveals another problem: in order to substitute the output data sets consisting of $\Delta T_j$, $T_{j,\min}$, and $t_{\text{on}}$ into (2), these sets need to be combined with the respective value of the bond-wire current. If the active time of a flow is split into different parts, these parts will not certainly occur with the same bond-wire current value. Therefore, it is not possible to have a representative current value that can be combined with the temperature and on-time conditions to give the correct

fatigue contribution. Possible solutions would be either to average out a current value corresponding to all the intervals that give the total value of the on-time, or maybe use always the nominal device current in the lifetime expression, but the calculation for the accumulated fatigue in each of these cases would be different (and most certainly inaccurate).

Given the statement in [2] that on-times below 1 s do not allow temperature gradients to fully develop, and thus, do not have significant contribution in fatigue, data sets containing on-times below this limit can be excluded from the fatigue calculation. Using the rainflow-counting algorithm on the original signal allows to identify these on-times, and excluding temperature variations with relatively small durations.

It can be observed from the shape of the device-temperature waveform in Fig. 6 that there is a significant amount of variations caused due to the fundamental-frequency current, which according to the reasoning presented above should not be considered as contributors to fatigue. Another supporting fact for this hypothesis is the following: The fundamental-frequency component in an electrical application develops temperature variations with on-times in the range of a few milliseconds. To give an estimation of these temperature variations, the datasheet characteristics of the investigated IGBT device can be considered. It is found that the junction-case transient thermal impedance for a time of 0.01 s is approximately 25% of its steady-state value (12.0 k/kW). This leads to a 9°C temperature rise for a 10-ms long conduction of the nominal current (1000 A) at 125°C ($V_{ce} = 3.1$ V). It is apparent that the mechanical forces caused by the fundamental-frequency components will most probably end up in the elastic range.

Power-cycling experiments are, anyway, not performed with on-times of a few milliseconds, but are rather based on slower transitions, starting in the best case from a few hundred milliseconds. As a result, there is no indication that a lifetime model, which is developed based on power-cycling experiments can describe accurately the fatigue contributions from fundamental-frequency temperature variations. Repeating the lifetime estimation process for the same waveform of the device T1 in Fig. 6, but this time ignoring the fatigue contributions from temperature variations with a duration below 10 ms, the estimated lifetime becomes 40.4 years.

### B. Effect of off-times

As already mentioned, rainflow counting can distinguish between heating and cooling transients, based on the type of source (peak or valley) each flow starts from. When a flow is closing, a half cycle is counted and characterised by the output data set of $\Delta T_j$, $T_{j,\min}$, and $\Delta t$ (which can be either ramp-up or ramp-down time).

The situation during power-cycling experiments is clear: The devices are cooling down with the current turned off, and the duration of these intervals is the necessary time for the device to cool down to the $T_{j,\min}$, before a new heating cycle starts. In this way, on-times, off-times, and the cyclic period are all related to each other. Therefore, in a model that describes lifetime during power-cycling experiments, it makes sense to use only on-times as the relevant parameter, both because all time-related parameters are strongly related to each other, and also because the bond-wire current value is zero during off-times. On-times are included in the lifetime expression in [2].

However, in field application conditions, the temperature waveform that is obtained has very different characteristics compared to the periodic waveform in power-cyclic experiments. In random variations, as shown in Fig. 6, negative $\Delta T_j$s (or cooling transients) can occur simply because the RMS current through a device is reduced (e.g. when the load current changes direction). It is unclear if the lifetime estimation should include these variations, and in what way can they be expressed in a formula like the one given in [2], where $t_{\text{on}}$ expresses heating times. To make this point more clear, two different possible interpretations are described in the following.

*1) Ignoring cooling transients:* As a first approach, it is assumed that damage occurs due to the temperature rise, and that each rise is followed by an equivalent temperature fall that will complete (at some point in the future) a full cycle. It does not matter what is the gradient of the cooling transient, as it is supposed to occur with zero current. Considering then that the damage occurring during a full temperature cycle is the damage caused by the heating transient (positive $\Delta T_j$), the useful output of the rainflow-counting algorithm is restricted to the flows sourced from valleys (positive gradient). Assuming that each such flow causes a full-cycle damage, the resulting lifetime when substituting the contributions into the lifetime formula for IGBT1 in Fig. 6 is 10.8 years (the same considerations were made for the result presented initially, in Section III).

*2) Considering damage from cooling transients:* Alternatively, it can be assumed that in field-application conditions, each temperature rise reflects only one half-cycle of damage, and that the negative temperature gradients contribute as half-cycles too. Negative temperature gradients can occur in field applications both with, and without current through the device. In case these are taken into account, substituting their duration as $t_{\text{on}}$ in the lifetime expression leads to the conclusion that different cooling gradients cause different damage contributions, even if their $\Delta T_j$s and the resulting minimum temperatures $T_{j,\min}$ are the same. If this consideration is true, application of the lifetime estimation process on the same data for IGBT1 in Fig. 6 estimates its lifetime now to 2.3 years.

It has to be pointed out here that the formula in [2] can distinguish temperature variations that occur with zero current, and exclude their fatigue contributions, while in [1] there is no such consideration. Among others that are discussed below, this is an extra degree of uncertainty, as different models treat the same observations in very different ways.

## VII. Impact of the Lifetime Model Selection

Until this point, the lifetime expression developed in [2] has been used, and coefficients to adapt this model to the specific device were adapted and presented in Table II. In a similar

way, the coefficients for the LESIT model [1] can be adapted as well, based on experience from power-cycling results on the 3.3-kV IGBT power module under investigation, as shown in Table IV. These coefficients can be used on the same rainflow-counting output data sets, to estimate the expected lifetime of the device T1, under the same load circumstances, but with another lifetime model this time.

TABLE IV
COEFFICIENTS OF THE ADAPTED LESIT MODEL FOR THE 3.3-KV IGBT POWER MODULE UNDER INVESTIGATION.

| $A$ | $\alpha$ |
|---|---|
| 6.289 | $-3.472$ |

The aforementioned cases are evaluated again, this time using the LESIT model, and the comparative results to the CIPS'08 model are presented in Table V.

TABLE V
LIFETIME ESTIMATION RESULTS USING DIFFERENT CONSIDERATIONS FOR TWO LIFETIME MODELS.

| | Adapted CIPS'08 [2] | Adapted LESIT [1] |
|---|---|---|
| Excluding variations in the elastic range | $\infty$ years | $\infty$ years |
| Excluding short on-times (fundamental-frequency cycles) | 40.4 years | 2.93 years |
| Considering only positive gradients | 10.8 years | 0.23 years |
| Considering both positive and negative gradients | 2.3 years | 0.23 years |

### A. Impact of the model coefficients used

The CIPS'08 model is developed using a large number of different device data. Running power-cycling experiments on a specific device, it is possible to obtain more accurate data to adapt the model (like the ones in Table IV), than interpolating data sourcing from many different devices. The coefficients presented in [2] are collected based on a large number of device data, as the purpose of this activity was to present all parameters that have an impact on lifetime estimation, and approximate their weight on the final result. Having a lifetime expression that indicates the important parameters can be used as a starting point, but the effect/weight of each parameter for a specific device may be different, depending on the device design. It is reasonable then to adapt the coefficients of this expression to reflect the properties of the specific device under consideration, as this will remove dependency from the device voltage class and bond-wire diameter. Applying the original parameters mentioned in [2], leads to estimated lifetimes as shown in Table VI.

## VIII. MINER'S RULE

Last but not least, even if the lifetime model would give a reliable indication of the damage contribution of each transient, there is a last process that linearly adds these contributions to estimate the accumulated fatigue, as in (3). However, this has not been confirmed to be the case for power devices, as there are no results in literature exposing devices to different stress profiles, and measuring the effect of each individual profile on the consumed lifetime. It is not certain that the sequence each stress profile occurs is independent of the damage contribution it creates.

TABLE VI
LIFETIME ESTIMATION RESULTS USING DIFFERENT PARAMETERS IN THE SAME LIFETIME MODEL.

| | Original CIPS'08 [2] | Adapted CIPS'08 |
|---|---|---|
| Excluding variations in the elastic range | $\infty$ | $\infty$ |
| Excluding short on-times (fundamental-frequency cycles) | 2.2 years | 40.4 years |
| Considering only positive gradients | 1.5 years | 10.8 years |
| Considering both positive and negative gradients | 0.7 years | 2.3 years |

Assuming that a device is exposed to a hard profile in the beginning of its life, with a periodic $\Delta T_j$ of 70°C at a $T_{j,\min}$ of 40°C. When half of its expected lifetime is consumed, the profile changes, and the $\Delta T_j$ is only 40°C, at the same $T_{j,\min}$, until the device reaches its end-of-life. Miner's rule suggests that changing the sequence of (or even interleaving) these profiles will result in the same overall lifetime. However, this is not verified in any previous literature for power devices, and cannot be taken for granted. Material fatigue is not necessarily a linear process, and should not be treated in this way, especially when random stress waveforms are apparent, which is the case in field applications.

## IX. GUIDELINES FOR LIFETIME ESTIMATION

It has been observed so far that a number of factors can cause significant inaccuracy in the estimation of accumulated damage on a power device. It should be stressed that despite pointing at these limitations, the aim of the paper is not to discredit the method that is still considered to be a recommended approach for lifetime calculation. In order to reduce the errors in this process, the aforementioned observations are consolidated and listed here in a number of guidelines to make correct application of the process in Fig. 1.

- All temperature variations that appear in the obtained temperature signal shall be included in the rainflow-counting process, and their contributions shall be evaluated only after the corresponding flows are closed. If there are flows with $\Delta T_j$s in the elastic range [24], they shall be excluded from the damage calculation.
- The temperature signal shall not be filtered in any way, but it shall be maintained in its original form. If only the signal reversals are kept (which is a common practice

in rainflow-counting for other engineering applications), then all information about on-times is lost.

- Closed flows with very short $t_{on}$ times shall be excluded from the fatigue calculation, as very short heating transients do not have an impact on the device damage. According to [2], in very fast transients, the temperature does not propagate through different material layers, and does not trigger the ageing mechanism.
- As the lifetime models are developed based on power-cycling experiments, where cooling down is not a regulated process, the fatigue caused in these experiments is mainly due to the characteristics of the heating transients. Consequently, only the data describing heating transients shall be substituted in these models, and their damage shall be calculated as full-cycle damage (not half-cycle damage, as indicated by the rainflow counting). Cooling transients (appearing in the output of the rainflow counting as flows sourcing from peaks) should be ignored.
- The coefficients of a lifetime model shall be adapted to characterize the specific device under investigation. The results presented in [1], [2] represent large number of different IGBT modules, in order to give a generic picture of their behaviour. However, individual modules may differ significantly from these averaged coefficients.
- The lifetime expression in (2) provides better accuracy in the estimation, as it involves more parameters. On the other hand, it should be applied carefully, and on the correct parameter values, as inappropriate application will give misleading results.
- Miner's rule needs further investigation to be verified or adapted appropriately to be useful for field application data. Applying a linear combination of all individual fatigue contributions is one approach, but in realistic conditions, appropriate margin should be kept from unity damage, in order to avoid unexpected failure situations.

## X. Conclusion

This paper has dealt with the factors that cause significant uncertainty to the lifetime estimation results for power devices. One device was selected and it has been tested in power-cycling experiments, to adapt the parameters of two lifetime models that are widely accepted in literature, in order to fit the device characteristics in the best way. The device has then been exposed to a certain load profile generated according to the conditions of a field application, and its junction temperature is estimated over the load variations.

This temperature, which does not vary in a periodic way, is processed using a methodology that seems sensible, in order to estimate the lifetime of the device under the given conditions in this application. It has been shown that the result of this methodology is very sensitive to a number of factors, which leads to high inaccuracy in the final estimation. One major factor is the lifetime model used for the estimation: Different models applied on the same data give very different results. Additionally, using a model that is representative for certain conditions, does not make it necessary applicable in every case. It has been shown that the coefficient values may be very different if the model is adapted to a certain device, compared to the general case. Last but not least, even when using the same lifetime formula with the exact same coefficient values, there is a number of different interpretations of a temperature waveform, each one of them giving very different results.

The aforementioned statements lead to the conclusion that there is no unambiguous way to interpret the temperature-waveform data into a lifetime expression, as these expressions are not meant to be used on field-application data. It needs to be stressed that statistical lifetime models can describe very well the behaviour of devices during power-cycling experiments, but it is not evident that they can give safe conclusions when applied on arbitrary application data.

## References

[1] M. Held, P. Jacob, G. Nicoletti, P. Scacco, and M. . Poech, "Fast power cycling test of igbt modules in traction application," in *Proceedings of Second International Conference on Power Electronics and Drive Systems*, vol. 1, May 1997, pp. 425–430 vol.1.

[2] R. Bayerer, T. Herrmann, T. Licht, J. Lutz, and M. Feller, "Model for power cycling lifetime of IGBT modules - various factors influencing lifetime," in *Proc. 5th Int. Conf. Integrated Power Electronics Systems*, Mar. 2008, pp. 1–6.

[3] J. Lutz, "IGBT-modules: Design for reliability," in *Proc. 13th European Conf. Power Electronics and Applications*, Sep. 2009, pp. 1–3.

[4] S. Schuler and U. Scheuermann, "Impact of test control strategy on power cycling lifetime," in *Proceedings of 2010 International Conference for Power Conversion Intelligent Motion (PCIM Europe)*, May 2010, pp. 355–360.

[5] H. Liu, K. Ma, Z. Qin, P. C. Loh, and F. Blaabjerg, "Lifetime estimation of mmc for offshore wind power hvdc application," *IEEE Journal of Emerging and Selected Topics in Power Electronics*, vol. 4, no. 2, pp. 504–511, June 2016.

[6] L. Wang, J. Xu, G. Wang, and Z. Zhang, "Lifetime estimation of IGBT modules for MMC-HVDC application," *Microelectronics Reliability*, vol. 82, pp. 90 – 99, 2018.

[7] M. Dbeiss, Y. Avenas, H. Zara, L. Dupont, and F. A. Shakarchi, "A method for accelerated aging tests of power modules for photovoltaic inverters considering the inverter mission profiles," *IEEE Trans. Power Electron.*, vol. 34, no. 12, pp. 12 226–12 234, Dec 2019.

[8] U. M. Choi, F. Blaabjerg, and S. Jørgensen, "Power cycling test methods for reliability assessment of power device modules in respect to temperature stress," *IEEE Trans. Power Electron.*, vol. 33, no. 3, pp. 2531–2551, Mar. 2018.

[9] H. Huang and P. A. Mawby, "A lifetime estimation technique for voltage source inverters," *IEEE Trans. Power Electron.*, vol. 28, no. 8, pp. 4113–4119, Aug 2013.

[10] M. Musallam, C. Yin, C. Bailey, and M. Johnson, "Mission profile-based reliability design and real-time life consumption estimation in power electronics," *IEEE Trans. Power Electron.*, vol. 30, no. 5, pp. 2601–2613, May 2015.

[11] L. R. GopiReddy, L. M. Tolbert, B. Ozpineci, and J. O. P. Pinto, "Rainflow algorithm-based lifetime estimation of power semiconductors in utility applications," *IEEE Trans. Ind. Appl.*, vol. 51, no. 4, pp. 3368–3375, 2015.

[12] C. Lalanne, *Fatigue Damage*. John Wiley & Sons, Ltd, 2014.

[13] M. Andresen and M. Liserre, "Impact of active thermal management on power electronics design," *Microelectronics Reliability*, vol. 54, no. 9-10, pp. 1935–1939, Sep.-Oct. 2014.

[14] J. Goncalves, D. J. Rogers, and J. Liang, "Submodule temperature regulation and balancing in modular multilevel converters," *IEEE Transactions on Industrial Electronics*, vol. 65, no. 9, pp. 7085–7094, 2018.

[15] F. Hahn, M. Andresen, G. Buticchi, and M. Liserre, "Thermal analysis and balancing for modular multilevel converters in HVDC applications," *IEEE Trans. Power Electron.*, vol. 33, no. 3, pp. 1985–1996, Mar. 2018.

[16] M. Matsuishi and T. Endo, "Fatigue of metals subjected to varying stress," *Japan Society of Mechanical Engineers*, vol. 68, no. 2, pp. 37–40, 1968.

[17] *Standard practices for cycle counting in fatigue analysis*, ASTM E 1049-85 (Reapproved 1997) Std.
[18] M. Musallam, C. M. Johnson, C. Yin, C. Bailey, and M. Mermet-Guyennet, "Real-time life consumption power modules prognosis using on-line rainflow algorithm in metro applications," in *2010 IEEE Energy Conversion Congress and Exposition*, Sept 2010, pp. 970–977.
[19] Y. Zhang, H. Wang, Z. Wang, Y. Yang, and F. Blaabjerg, "Impact of lifetime model selections on the reliability prediction of igbt modules in modular multilevel converters," in *2017 IEEE Energy Conversion Congress and Exposition (ECCE)*, Oct 2017, pp. 4202–4207.
[20] M. A. Miner, "Cumulative damage in fatigue," *Journal of Appl. Mech.*, vol. 12, no. 3, pp. A159–A164, Sep. 1945.
[21] A. Antonopoulos, S. D'Arco, M. Hernes, and D. Peftitsis, "Challenges and strategies for a real-time implementation of a rainflow-counting algorithm for fatigue assessment of power modules," in *2019 IEEE Applied Power Electronics Conference and Exposition (APEC)*, March 2019, pp. 2708–2713.
[22] C. Herold, J. Franke, R. Bhojani, A. Schleicher, and J. Lutz, "Methods for virtual junction temperature measurement respecting internal semiconductor processes," in *2015 IEEE 27th International Symposium on Power Semiconductor Devices IC's (ISPSD)*, May 2015, pp. 325–328.
[23] J. Lutz, H. Schlangenotto, U. Scheuermann, and R. D. Doncker, *Semiconductor Power Devices: Physics, Characteristics, Reliability*. Springer Berlin Heidelberg, 2011.
[24] S. Hartmann and E. Özkol, "Bond wire life time model based on temperature dependent yield strength," in *Proceedings of 2012 International Conference for Power Electronics, Intelligent Motion, Power Quality and Energy Management (PCIM Europe)*, 8-10 May 2012, pp. 494–501.

**Antonios Antonopoulos** (S'06, M'15) was born in Athens, Greece, in 1984. He received the Diploma on Electrical and Computer Engineering from the National Technical University of Athens, Greece in 2007, and his Licentiate and PhD degrees on Power Electronics from the KTH Royal Institute of Technology, in Stockholm, Sweden in 2011 and 2015 respectively.

Between 2014 and 2017 he worked at the department of Electrical Systems, at ABB Corporate Research Center, in Västerås, Sweden. In 2018 he was a guest researcher at the Norwegian University of Science and Technology (NTNU) in Trondheim, Norway. He is currently an Assistant Professor on Power Electronics at the National Technical University of Athens, where he serves since the fall of 2018. His research interests include design, control, and reliability aspects of high-power-electronic converters for large- and medium-scale motor drives and grid applications.

**Salvatore D'Arco** received the M.Sc. and Ph.D. degrees in Electrical Engineering from the University of Naples "Federico II," Naples, Italy, in 2002 and 2005, respectively.

From 2006 to 2007, he was a postdoctoral researcher at the University of South Carolina, Columbia, SC, USA. In 2008, he joined ASML, Veldhoven, the Netherlands, as a Power Electronics Designer consultant, where he worked until 2010. From 2010 to 2012, he was a postdoctoral researcher in the Department of Electric Power Engineering at the Norwegian University of Science and Technology (NTNU), Trondheim, Norway. In 2012, he joined SINTEF Energy Research where he currently works as a Research Scientist. He is the author of more than 100 scientific papers and is the holder of one patent. His main research activities are related to control and analysis of power-electronic conversion systems for power system applications, including real-time simulation and rapid prototyping of converter control systems.

**Magnar Hernes** received the M.Sc. degree in Electrical Engineering at the Norwegian University of Science and Technology in 1977. He is senior research scientist at SINTEF Energy Research where he has been employed since 1979. He has broad experience from development of power electronics products for the industry. He has conducted several research programs within power electronics, like power electronics for grid integration, drive systems for electrical vehicles, power electronics for the renewable industry, and pressure tolerant power electronics for subsea oil and gas exploitation.

**Dimosthenis Peftitsis** (Senior Member, IEEE) is Associate Professor of Power Electronics in the Department of Electrical Power Engineering at the Norwegian University of Science and Technology (NTNU) in Trondheim, Norway where he has been a faculty member since May 2016.

Born in Kavala, Greece, he received his Diploma degree (Hons.) in Electrical and Computer Engineering from Democritus University of Thrace (Xanthi, Greece) in 2008. In his final year of studies, he spent six months in ABB Corporate Research, Västerås, Sweden, writing his thesis. He completed his Ph.D. degree at the KTH Royal Institute of Technology (Stockholm, Sweden) in 2013. Dimosthenis was a Postdoctoral Researcher involved in the research on SiC converters at the Department of Electrical Energy Conversion, KTH Royal Institute of Technology (2013-14). He also worked as a Postdoctoral Fellow at the Lab for High Power Electronics Systems, ETH Zurich, where he was involved in dc-breakers for multiterminal HVDC systems (2014 to 2016).

His research interests lie in the area of power converters design using WBG devices (e.g. SiC, GaN) including adaptive drive circuits, dc-breaker design for MV and HVDC systems, as well as reliability assessment and lifetime modelling of high-power semiconductor devices, including reliability of SiC power switches. He has published more than 60 journal and conference papers; he is the co-author of one book chapter and the presenter of 5 conference tutorials. Dimosthenis is a member of the Outstanding Academic Fellows Programme at NTNU, a member of the EPE International Scientific Committee and currently serves as the Chairman on the Norway IEEE joint Power Electronics Society/Industry Applications Society/Industrial Electronics Society Chapter.